

## Classification

Physics Abstracts

82.50Gw—61.80Fe—71.30+h—72.80Ga

## Direct Measurements of the Radiolytic Transformation of Thin Films of Titanium Dioxide using EELS

Peter Rez<sup>(1)</sup>, Jon Karl Weiss<sup>(2)</sup>, Douglas L. Medlin<sup>(3)</sup> and David G. Howitt<sup>(4)</sup>

<sup>(1)</sup> Center for Solid State Sciences and Department of Physics, Arizona State University, Tempe AZ 85287-1704, U.S.A.

<sup>(2)</sup> EMISPEC, 2409 South Rural Road, Tempe AZ 85287-1704, U.S.A.

<sup>(3)</sup> Sandia National Laboratories, Physical Properties of Material Department, Livermore, CA 94551, U.S.A.

<sup>(4)</sup> Department of Chemical Engineering and Materials, Science University of California, Davis, CA 95616, U.S.A.

(Received August 17; accepted September 30, 1995)

**Abstract.** — The reduction of TiO<sub>2</sub> (anatase) subjected to high flux electron irradiation ( $\sim 10^8$  A/m<sup>2</sup>) to titanium monoxide is followed using the evolution of fine structure in the electron energy loss spectrum. Changes in extended fine structure are consistent with changes in interatomic distance and the shift in d band onset clearly shows the transition from insulator to metal.

### 1. Introduction

The electron radiation damage of metal oxides is of interest for applications in nanolithography. Many oxides are insulators, and thus the damage in these materials can be due to ionization damage, field induced migration, knock-on displacement, or a combination of these effects.

In some cases knock-on displacement clearly plays a role, and this can often be identified from the anisotropy of the effect. In MgO, for instance, (001) faceted holes are observed to grow in from the electron exit surface at a rate proportional to beam flux when thin foils of the material are irradiated at high current densities ( $10^6 - 10^8$  A/m<sup>2</sup>) [1, 2]. Although the directionality of the hole growth verifies the role of sputtering, a calculation of the energy necessary for this process rules out a simple momentum transfer. The unrelaxed energy to create an anion or cation vacancy in the (001) surface of MgO has been calculated, using pair potentials, to be about 40 eV [3]. This energy corresponds to sputtering thresholds for oxygen and magnesium of 240 and 330 keV respectively and in contrast, the low energy (40 keV) at which this effect occurs indicates that the binding energies for oxygen and magnesium must be less than 5.7 and 3.8 eV, respectively. Turner *et al.* [1] have suggested that such low thresholds could arise if the surface were hydroxylated or if sputtering were occurring from low coordination sites on the surface of the growing hole.

In several other oxides it appears that a radiolytic mechanism is responsible for the initial damage. Knotek and Feibelman [4, 5] have described an ionization damage process that occurs at the surfaces of maximally valent oxides (i.e., oxides in which the metal ion is ionized to its noble

gas configuration). Following the ionization of a deep core level on the cation in these materials, an electron from the oxygen valence shell decays to fill the resulting hole on the cation releasing sufficient energy to remove, by Auger emission, two additional electrons from the oxygen anion. Thus, the oxygen ion loses a total of three electrons giving it a net charge of +1. The resulting  $O^+$  ion will be ejected if it is near the surface because of the coulombic repulsion of the surrounding metal ions.

Using high resolution transmission electron microscopy (HRTEM), McCartney and Smith [6] studied the response of several maximal valence transition metal oxides ( $Nb_2O_5$ ,  $V_2O_5$ ,  $TiO_2$ , and  $WO_3$ ) to electron irradiation. At intermediate current densities of  $10^5 - 10^6$  A/m<sup>2</sup> and irradiation times on the order of 10 - 30 minutes, only the first few surface layers are depleted of oxygen. The damage apparently continues until the surface phases are reduced to the monoxide and is similar to earlier HRTEM observations of  $V_2O_5$  reduction [7]. McCartney and Smith interpreted the damage as arising from the interatomic Auger decay mechanism and pointed out that because the resulting monoxides are conductors further ionization damage would be suppressed. However, at higher current densities ( $10^7 - 10^8$  A/m<sup>2</sup>) even the monoxides of titanium can be reduced [8-10]. Crozier *et al.* [9] utilizing the contrast from secondary electrons emitted from the top and bottom surfaces of an electron irradiated thin foil, observed that this subsequent damage occurred preferentially at the electron exit surface, indicating that an electron momentum transfer mechanism must be responsible. Garvie and Craven [11] showed the reduction of  $Mn^{4+}$  to  $Mn^{2+}$  in the mineral asbolan using changes in EELS fine structure.

During radiation damage the interatomic distances and the coordination of titanium around the oxygen change. The most significant change is that the material transforms from an insulator to a metal. Earlier EELS work [12] showed how the fine structure on both the oxygen and titanium edges was related to the  $t_{2g}$  and  $e_g$  molecular orbitals. Some results showing the effects of beam damage on reflection core loss spectra of  $TiO_2$  have been published [13]. In this paper we show how the changes in bonding and interatomic distance can be followed from changes in the extended fine structure during time resolved EELS. We also show the shift in the conduction band states corresponding to an insulator to metal transition.

## 2. Experimental

Thin  $TiO_2$  films (50 nm thick) were prepared by reactive ion deposition on single crystal NaCl substrates. The initially amorphous films were annealed for twenty minutes at 500 °C to induce crystallization to anatase, with a grain size on the order of microns, and thereby ensuring stoichiometry [14]. These films were subsequently irradiated *in situ* in a 100 keV Philips 400 electron microscope using a field emission source. Irradiations were performed in areas of defect free, crystalline anatase, with a 10.5 nA probe of 10 nm diameter giving a current density at the specimen of  $1.3 \times 10^8$  A/m<sup>2</sup>. The changes in the energy loss spectra in the region of the Ti  $L_{2,3}$  edge and the oxygen K edge were recorded in real time using a Gatan 666 parallel electron energy loss spectrometer (PEELS) controlled by a specialized data acquisition system [15]. The acquisition time for each spectrum was 1 s and the damage was followed for a period of 5 min.

## 3. Results and Discussion

The spectra in Figure 1 show the region of energy loss between the Ti  $L_{2,3}$  and oxygen K edges. The upper line represents the first few spectra that were recorded prior to the onset of visible damage and the lower line, the spectrum from the damaged material. Key features to note are

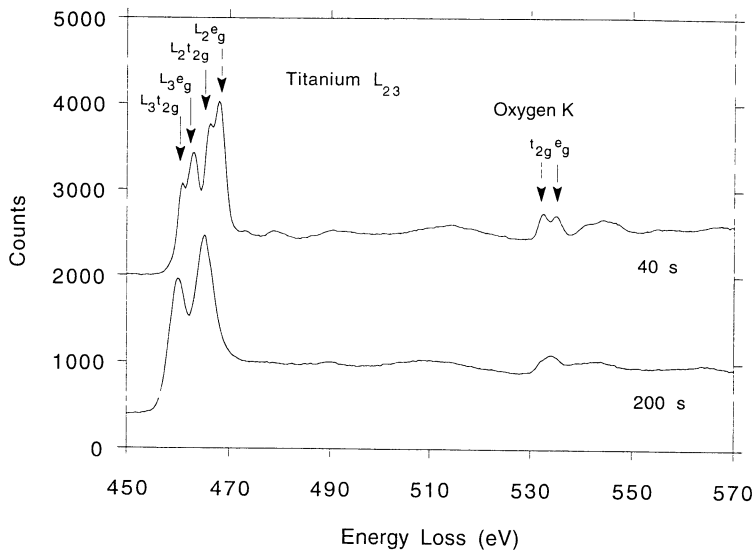


Fig. 1. — Comparison of the energy loss from spectra obtained prior to the onset of visible damage (40 s) and after irradiation for 200 s.

the changes in the form of the Ti  $L_{23}$  white lines and the fine structure on the oxygen K edge. In the original undamaged material the white lines are split into two components ( $t_{2g}$  and  $e_g$  peaks) as is the peak at the oxygen threshold. This splitting is the crystal field splitting and comes about because of the octahedral symmetry of the Ti ions. The  $t_{2g}$  components represent anti-bonding  $\pi^*$  states and the  $e_g$  components represent antibonding  $\sigma^*$  states of higher energy.

On the Ti  $L_{23}$  edge it is also apparent that the splitting between the  $t_{2g}$  and  $e_g$  components disappears as the irradiation damage proceeds. This is a reproducible effect and indicates the change in the bonding of the Ti atoms. What is more significant is the shift in  $L_3$  threshold position from 459.1 eV to 457.3 eV. The white line components represent transitions to the lowest part of the conduction band which is principally composed of the Ti d states with some mixing from the oxygen p states. This would indicate a shift downwards in the conduction band, consistent with the material transforming from an insulator to a metal (or more likely semimetal) in a manner consistent with a reduction from  $\text{TiO}_2$  to  $\text{TiO}$  or indeed to titanium metal.

In Figure 2, which shows the oxygen K edge, it is apparent that the two peak threshold, again corresponding to  $t_{2g}$ ,  $e_g$  orbitals, has reduced to a single peak at threshold. There also appears to be a loss of oxygen and the extended fine structure has changed. The peaks marked A and B in Figure 2 are shifted to lower energies and the peak marked B has only one peak in the spectrum from the damaged material (compared to two peaks in the undamaged). A full listing of peak positions is given in Table I. Comparison with the results of Brydson *et al.* [12] and Manoubi [16] shows that the fine structure of the undamaged material bears more resemblance to the fine structures of rutile rather than anatase. A closer examination of the damage in the first few seconds, shown in Figure 3, shows a change from the 2 peak extended structure of anatase to the 3 peak structure characteristic of rutile. It is notable that there is no shift of the threshold during the course of the damage. This is because the states contributing (i.e., the p-like states at the oxygen site) do not represent the bottom of the conduction band in the damaged material.

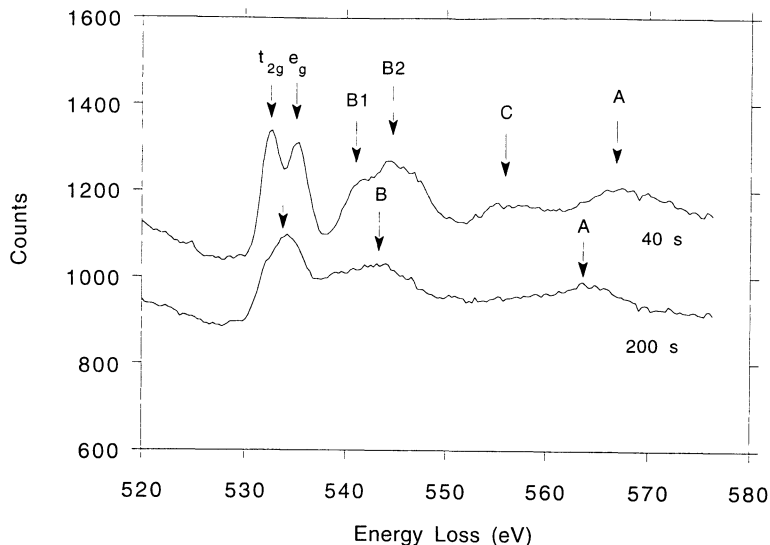


Fig. 2. — Oxygen K edge before and after damage. Note change in the two-peak threshold corresponding to the  $t_{2g}$  and  $e_g$  orbitals. Note also the changes in the peaks marked A, B, and C.

Table I. —  $TiO_2$  Energies are  $\pm 1$  eV. (\*)

Titanium L <sub>23</sub>		Oxygen K	
Feature	Energy (eV)	Feature	Energy (eV)
threshold	459.1	threshold	530.9
L <sub>3</sub> t <sub>2g</sub>	459.9	t <sub>2g</sub>	531.9
L <sub>3</sub> e <sub>g</sub>	462.1	e <sub>g</sub>	534.7
L <sub>2</sub> t <sub>2g</sub>	465.4	1st shoulder (B1)	540.8
L <sub>2</sub> e <sub>g</sub>	467.2	1st peak (B2)	543.7
little peak (A)	472.2	2nd peak (C)	556.8
1st big peak (B)	477.3	3rd peak (A)	566.6
2nd peak (C)	489.5		
3rd peak (D)	513.5		

(\*) Note: Although the absolute values of the energies may be associated with a small error, the relative energies between the spectral features from the anatase and the radiation damaged materials are quite precise.

The general shape of the oxygen K edge of the damaged material is typical of oxygen K edges found in materials with the sodium chloride structure such as MgO, SrO, CaO and BaO. The peak, marked A, can be identified as the 1st EXAF peak, and it arises from the backscattering from nearest neighbor oxygen atoms [17]. The shift to lower energy with damage indicates an increase in the average oxygen - oxygen distance. The energy separation of peak A from threshold was measured in the spectra from damaged and undamaged material. The threshold was taken to be the channel corresponding to half the increase in intensity at the edge, and the peak maximum was taken to correspond to the channel of maximum intensity. As the phase shifts remain the same

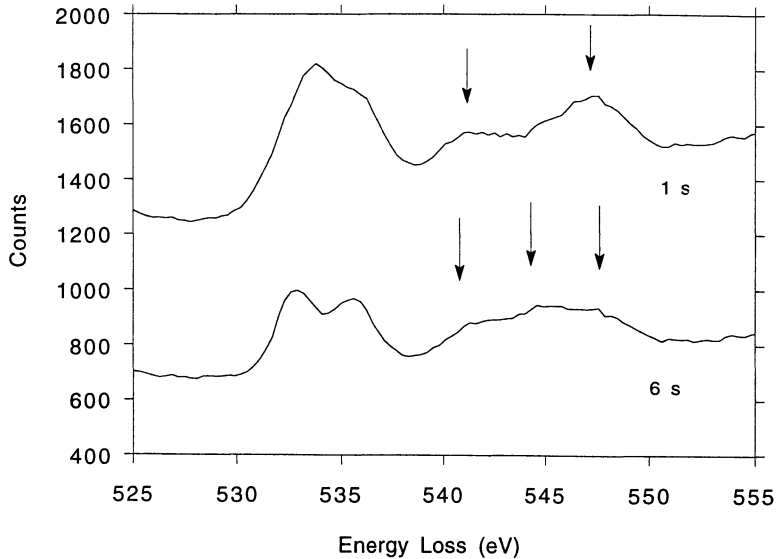


Fig. 3. — Oxygen K edge from spectra taken after 1 s and 6 s showing the change from the 2 peak structure of anatase to the 3 peak structure of rutile.

Table II. — *Damaged Materials; (TiO) Energies are  $\pm 1$  eV.*

Titanium L <sub>23</sub>		Oxygen K	
Feature	Energy (eV)	Feature	Energy (eV)
threshold	457.3	threshold	530.9
L <sub>3</sub>	459.1	peak	533.1
L <sub>2</sub>	464.3	1st peak (B)	542.8
little peak (A)	gone	2nd peak (C)	gone
1st peak (B)	gone	3rd peak (A)	564.4
2nd peak (C)	489.5		
3rd peak (D)	508.4		

the interatomic distance can be extracted from the relationship  $\sqrt{E} \cdot r = \text{constant}$ . A quantitative analysis using the values given in the Table shows a 3.5% increase. Peak B is probably due to scattering from the 2nd coordination shell, or possibly mixed scattering from the 1st and 2nd shells combined [17]. The change from a doublet peak to a singlet structure is indicative of the difference in bonding in the radiation damaged material. This is also apparent from a detailed analysis of the Ti L<sub>23</sub> extended structure. Figure 4 shows the inward shift of peak D which is also consistent with the increase in distance, although it should be stressed that this interpretation is by no means conclusive. For example, no account has been taken of the difference between the L<sub>3</sub> and L<sub>2</sub> fine structures, the complexity of the L<sub>1</sub> edge, or the uncertainty of a determination of the zero of energy to the extended structure. It should be pointed out, however, that the disappearance of the other features in Figure 4 can also be attributed to the increase in symmetry.

Finally, Figure 5 shows the measured change in oxygen content as the radiation damage proceeded during a second time series with lower total dose. Conventional background subtraction, such as  $AE^{-r}$ , does not work because of the short distance between the Ti L<sub>23</sub> and oxygen K

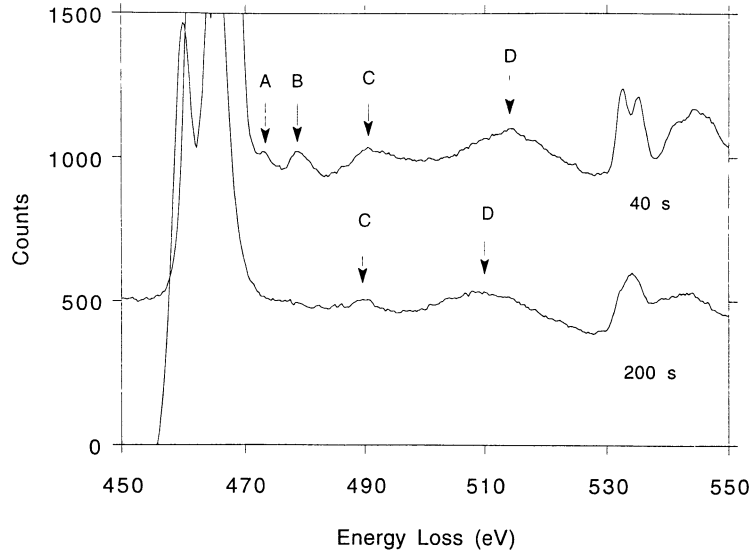


Fig. 4. — Titanium L<sub>23</sub> extended structure.

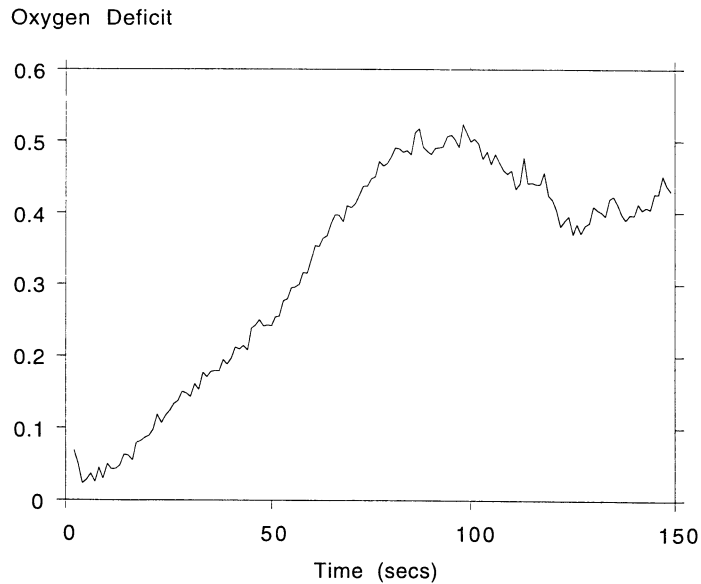


Fig. 5. — Oxygen deficit,  $x$ , assuming stoichiometry  $\text{TiO}_{2-x}$  as function of time for a 2nd, lower dose, damage series.

edges and the magnitude of the fine structure on the titanium edge. In order to remove the background contribution in Figure 5 we performed an  $AE^{-r}$  fit before the titanium edge, extrapolated the fit well beyond the oxygen edge, normalized the spectrum to the first spectrum in the series using a region free of fine structure between 500 eV and 520 eV, and then took the difference in

counts from the oxygen region between the current spectrum and the first spectrum. The oxygen/titanium ratios were quantified using calculated Hartree-Slater cross sections [18, 19]. If the chemical formula for damaged material is represented as  $TiO_{2-x}$  the deficit in oxygen content,  $x$ , will appear as an increase in Figure 5. The results are rather noisy, which we believe is due to the nonuniformity of the damage. In this case the end product is  $TiO_{1.38}$ , however an analysis of the series, whose fine structure is shown in Figures 1 to 4, gives an end product of  $TiO$ . These results are consistent with the findings of McCartney and Smith [6] who note a transformation to the sodium chloride structure and an increase of about 5% in the oxygen-oxygen separation during the high resolution electron microscopy of  $TiO_2$ .

#### 4. Conclusions

We have shown how time-resolved parallel EELS spectroscopy can be used to follow the beam-induced transition of anatase ( $TiO_2$ ) to  $TiO$ . The insulator-metal transition can be clearly seen as a shift in the  $Ti L_{2,3}$  threshold. This edge arises from transitions to the lowest unoccupied conduction band states which are mainly  $Ti d$  orbitals. Changes in bonding are readily apparent from the disappearance of the splitting due to the  $t_{2g}$  and  $e_g$  orbitals. Analysis of shifts in the oxygen extended fine structure is consistent with a 3.5% change in the oxygen-oxygen bond distance. Changes in the oxygen fine structure in the first few seconds of damage are indicative of a transformation from anatase to rutile. Using a novel method for background subtraction it was shown that the material remaining after damage was  $TiO$ . We have also demonstrated that these changes can be followed in real time using PEELS and a specialized data acquisition system

#### Acknowledgements

Support for this work was provided by the Department of Energy from the Office of Basic Energy Science under contract DE-FG03-86ER45279. The use of equipment at the National Center for High Resolution Electron Microscopy supported by the National Science Foundation under grant DMR 911-5680 is also acknowledged. P.R. would also like to acknowledge support from NSF grant DMR 930-6253.

#### References

- [1] Turner P. S., Bullough T. J., Devenish R. W., Maher D. M. and Humphreys C. J., *Philos. Mag. Lett.* **61** (1990) 181.
- [2] Devenish R. W., Bullough T. J., Turner P. S. and Humphreys C. J., Electron Beam Machining of  $MgO$  and  $ZnO$  in the STEM (Institute of Physics, Bristol, 1989) p. 267.
- [3] Duffy D. M., Hoare J. P. and Tasker P. W., *J. Phys. C: Solid State Physics* **17** (1984) L195.
- [4] Knotek M. L. and Feibelman P. J., *Phys. Rev. Lett.* **40** (1978) 964.
- [5] Knotek M. L. and Feibelman P. J., *Surf. Sci.* **90** (1979) 78.
- [6] McCartney M. R. and Smith D. J., *Surf. Sci.* **221** (1989) 214.
- [7] Fan H. J. and Marks L. D., *Ultramicrosc.* **31** (1989) 57.
- [8] Berger S. D., Macaulay J. M. and Brown L. M., *Philos. Mag. Lett.* **56** (1987) 179.
- [9] Crozier P. A., McCartney M. R. and Smith D. J., *Surf. Sci.* **237** (1990) 232.
- [10] McCartney M. R., Crozier P. A., Weiss J. K. and Smith D. J., *Vacuum* **42** (1991) 301.
- [11] Garvie L. A. J. and Craven A. J., *Ultramicrosc.* **54** (1994) 83.

- [12] Brydson R., Williams B. G., Engel W., Sauer H., Zeitler E. and Thomas J. M., *Solid State Commun.* **64** (1987) 609.
- [13] Wang Z. L., Liu J. and Cowley J. M., *Surf. Sci.* **216** (1989) 528.
- [14] Howitt D. G. and Harker A. B., *J. Mater. Res.* **2** (1987) 201.
- [15] Weiss J. K., Rez P. and Higgs A. A., *Ultramicrosc.* **41** (1992) 291.
- [16] Manoubi T., Thèse, Docteur es Sciences (Université Paris-Sud, 1989).
- [17] Rez P., Weng X. and Ma H., *Microsc. Microanal. Microstruct.* **2** (1991) 143.
- [18] Leapman R. D., Rez P. and Mayer D. T., *J. Chem. Phys.* **72** (1980) 1232.
- [19] Ahn C. C. and Rez P., *Ultramicrosc.* **17** (1985) 105.